Supporting information for:

Integrating recombinase polymerase amplification with CRISPR/Cas9-initiated nicking-rolling circle amplification in *Staphylococcus aureus* assay

Experimental section

Materials and reagents

Lysozyme (>20 KU/mg), Tap DNA polymerase (5 U/μL) with 10× Taq DNA polymerase buffer (100 mM Tris-HCl, 500 mM KCl, 15 mM $MgCl_2$, 0.8% (v/v) NonidetP40; pH=8.8 at 25 ℃), T4 DNA ligase (5 U/μL) with 10× T4 ligation buffer (400 mM Tris, pH 7.8, 100 mM $MgCl_2$, 100 mM DTT, 10 mM ATP), T7 RNA polymerase (50 U/μL) with 5×T7 transcription buffer (200 mM Tris-HCl, 30 mM $MgCl_2$, 50 mM DTT, 50 mM NaCl, 10 mM spermidine; pH=7.9 at 25 ℃), deoxyribonuclease I (DNase I, 1 U/μL) with 10× Reaction Buffer (100 mM Tris-HCl, 25 mM $MgCl_2$, 1 mM $CaCl_2$; pH=7.5 at 25℃), RNase inhibitor (40 U/μL), deoxynucleotide triphosphates (dNTPs, 10 mM), NTP set (100 mM each, nuclease free), Cas9 nuclease (SpCas9, 1 μM) with 10×Cas9 reaction Buffer (500 mM Tris-HCl, 1 M NaCl, 100 mM $MgCl_2$, 1 mg/mL BSA; pH=7.9 at 25℃) and 10000×SYBR Green I were ordered from Beyotime Biological Technology Co., Ltd. (Shanghai, China). RPA was performed using the GenDx Basic kit purchased from GenDx Biotech Co. Ltd. (Suzhou, China). The 10× NEbuffer 2 (500 mM NaCl, 100 mM $MgCl_2$, 100 mM Tris-HCl, 10 mM DTT; pH=7.9), Klenow fragment polymerase (3'-5' exo-, 5 U/μL), 10× CutSmart buffer (200 mM Tris-acetate, 100 mM magnesium acetate, 500 mM potassium acetate, and 1 mg/mL BSA; pH=7.9), and Nt. BbvCI endonuclease (10 U/μL) were provided by New England Biolabs Co., Ltd (Beijing, China). The tris-buffer (10 mM Tris−HCl, 100

mM NaCl, and 10 mM $MgCl_2$; pH=8.2), 30% acrylamide: bis-acrylamide (29:1), N,N,N',N'-Tetramethylethylenediamine (TEMED), ammonium persulfate (AP), 1× TBE electrophoresis buffer (90 mM Tris, 90 mM boric acid, 10 mM EDTA, and 7 M urea; pH=8.0), 10×DNA loading buffer and deoxynucleotide triphosphates (dNTPs, 10 mM) were provided by Servicebio Biotechnology Co., Ltd. (Wuhan, China). The oligonucleotides (**Table S1**) and ThT were provided by Sangon Biotech Co. Ltd. (Shanghai, China). Ultrapure water (Resistance=18.2 MΩ) produced from a Milli-Q Water Purification System (Millipore, USA) was used in this study.

Instruments

Fluorescence measurements were carried out utilizing a PerkinElmer FL8500 Fluorescence Spectrophotometer (Waltham, USA). The parameters were set as follows: an excitation wavelength of 430 nm, slit widths of 10/10 nm, scanning speed of 1200 nm/min, recording range spanning 450-600 nm, and a PMT detector voltage set to 650 V. For electrophoresis experiments, a Servicebio PW-600 electrophoresis analyzer (Wuhan, China) was employed. Gel imaging was achieved using a ChampGel 7000 gel imaging system (Beijing, China). The pH values of buffers were determined using a LeiCi PHS-3E desktop pH meter (Shanghai, China). The control of a constant reaction temperature of RPA was achieved using a Bio-Rad T100 thermal cycler system (Hercules, USA).

Circular Dichroism (CD) Measurements

CD spectra was performed on a JASCO J-1700 CD spectrometer (Tokyo, Japan) at room temperature. Three scans were accumulated and averaged under the following conditions: range from 200 to 500 nm, speed of 200 nm/min, response time of 0.5 s, bandwidth of 1.0 nm, and quartz cuvette of 0.1 cm path length. The samples were prepared by using 10 μM G-rich oligomers in the absence and presence of ThT (100 μM) in Tris-buffer (25 mM, pH 7.4, 50 mM of KCl) and incubating at room temperature

for several hours.

Melting Curves

The melting curve study was carried out on a JASCO J-1700 CD spectrometer (Tokyo, Japan) equipped with a Peltier temperature controller. Normalized CD melting curves of di-G-triplex and di-G-triplex/ThT compound recorded at 265 nm under the following conditions: range from 20 to 90 °C, scan rate of 3 °C/min, fentes band width of 1 nm, and quartz cuvette of 1 cm path length. The samples were prepared by using 5 μM di-G-triplex oligomer in the absence and presence of ThT (25 μM) in Tris-buffer (25 mM, pH 7.4, 50 mM of KCl).

Fluorometric titrations

Fluorometric titrations of ThT with mono-G-triplex or di-G-triplex^{A} were per-formed in the Tris-buffer used for binding as mentioned above. For the assay, the ThT (200 nM) was mixed with mono-G-triplex or di-G-triplex^{A} at different concentrations (0.05, 0.1, 0.2, 0.3, 0.4, 0.5, 0.6, 0.7, and 0.8 μM). After leaving the mixtures to stand for 30 min at room temperature in the dark, fluorescence spectra were collected. The data from the fluorometric titrations were analyzed according to the independent-site model by nonlinear fitting to Equation (1),[1, 2] in which F_0 is the background fluorescence intensity of ThT in the absence of DNA, F_{max} is the fluorescence intensity upon saturation, n is the putative number of ThT molecules binding to a given DNA strand and K_D is the apparent equilibrium dissociation constants. The parameters Q and A were evaluated by a Levenberg–Marquardt fitting routine in OriginPro 2021 software.

$$\frac{F}{F_0} = 1 + \frac{Q-1}{2}\left[A + 1 + x - \sqrt{(A+1+x)^2 - 4x}\right]\#() \quad 1.$$

$$A = \frac{1}{K_D\, C_{ThT}}, x = n\frac{C_{DNA}}{C_{ThT}}, Q = \frac{F_{max}}{F_0}$$

Preparation of sgRNA

Initially, the long DNA template utilized for RNA transcription was synthesized through the combination of a scaffold template (5 μM, 2 μL), primer for the scaffold template (5 μM, 2 μL), and target-specific template (5 μM, 2 μL), with the involvement of Tap DNA polymerase (5 U/μL, 1 μL), 10× Taq DNA polymerase buffer (2 μL), dNTPs (10 mM, 1 μL), and 10 μL of ddH_2O. The amplification process followed these conditions: 94 °C for 3 min, succeeded by 30 cycles at 94 °C for 30 s, 55 °C for 30 s, and 72 °C for 1 min. Subsequently, the resultant double-stranded long DNA template for sgRNA transcription underwent a 10 min incubation at 72 °C, succeeded by a cooling step to 4 °C. In a 20 μL transcription system, 5 μL of long DNA template for sgRNA, 5 μL of 1 μM T7 RNA polymerase, 4 μL of 5× T7 transcription buffer, 1 μL of RNase inhibitor (40 U/μL), 2 μL of 100 mM NTPs, and 3 μL of ddH_2O were introduced and incubated at 37 °C for a span of 9 h. Ultimately, 4 μL of DNase I (1 U/μL), 3 μL of 10× Reaction Buffer, and 3 μL of ddH_2O were supplemented, undergoing a 9-h incubation at 37 °C to digest any residual DNA template. The resulting products were then stored at –80 °C for subsequent utilization.

Bacterial Culture and Extraction of Genomic DNA

S. aureus was cultivated and growth within a Luria-Bertani (LB) medium at a temperature of 37°C for 24 h in a controlled shaking incubator. Subsequently, the concentration of *S. aureus w*as determined through the conventional plate-counting method. The solution containing *S. aureus* underwent centrifugation at 3000 rpm for a duration of 10 min to eliminate the culture medium. The resultant *S. aureus* was subjected to serial dilution using 1× PBS, generating concentrations spanning from 1 to 10^9 CFU/mL. Extraction of total DNA from *S. aureus w*as obtained using the Bacterial Genome DNA Extraction Kit by Tiangen Biotech Co., Ltd. (Beijing, China), following the manufacturer's protocol.

Extraction of Genomic DNA from blood

Isolation of *S. aureus* from blood was achieved using a separation medium with a density of 1.077 g/mL (20ºC), purchased from Beyotime Biological Technology Co., Ltd. (Shanghai, China). Initially, blood samples containing *S. aureus* were diluted with saline in a 2:1 ratio at room temperature. The diluted sample was then gently added to a centrifuge tube containing 5 mL of the separating medium. Subsequently, the sample underwent centrifugation at 500 g for 25 min at a temperature of 20 °C. Following centrifugation, the transparent layer of liquid, which contained *S. aureus,* was carefully and slowly extracted. Total DNA extraction from *S. aureus* was performed using the Bacterial Genome DNA Extraction Kit by Tiangen Biotech Co., Ltd. (Beijing, China), following the manufacturer's protocol.

RPA-CRISPR/Cas9-nRCA based *S. aureus* detection

To perform the RPA-CRISPR/Cas9-nRCA, the RPA process was conducted as follows: At first, the lyophilized powder containing polymerase and recombinase was completely dissolved by 20 μL of solvent. Then, 24 μL of ddH_2O, 1 μL of forward primer (FP) at 10 μM, and 1 μL of reverse primer (RP) at 10 μM were introduced and thoroughly mixed. The resulting solution was divided into two separate tubes, each designated for the positive RPA and negative controls. In the positive tube, 1 μL of genomic DNA sourced from *S. aureus* and 1 μL of activator (magnesium acetate) were incorporated. The negative control tube followed identical procedures, with the exception of substituting the DNA template with ddH_2O. Of note, all operations were conducted in a sterile and cool environment to ensure sample addition and reaction stability. For the CRISPR/Cas9-nRCA process, 2 μL of 1 μM Cas9, 2 μL of 10× Cas9 Reaction Buffer, 2 μL of 1 μM sgRNA, and 1 μL of RNase inhibitor (40 U/μL) were combined and incubated at 25 ℃ for 10 min. Next, 2 μL of the RPA product and 11 μL of ddH_2O

were introduced into the mixture, undergoing incubation at 37 °C for 1 h. Following this, an additional 3 μL of ddH_2O, 2 μL of 5 μM padlock probe, 2 μL of T4 DNA ligase (5 U/μL), and 3 μL of 10× T4 ligation buffer were sequentially incorporated. After an incubation at 16 °C for 30 min, 0.8 μL of Klenow fragment (5 U/μL), 5 μL of 10× NEBuffer 2, 1 μL of Nt. BbvCI (10 U/μL), 5 μL of 10× CutSmart, 1 μL of 10 mM dNTPs, and 7.2 μL of ddH_2O were added in sequence to initiate the nRCA process at 37℃ for 1 h. Finally, the reaction was terminated at 65 ℃ for 10 min. The resultant 50 μL sample was mixed with 130 μL ddH_2O and 20 μL of Tris buffer (500 mM, pH = 7.4) containing 1 μM NaCl and 10 μM ThT. Following a 60 min reaction at 37 °C, the solution was transferred to a microcuvette for subsequent fluorescence recording.

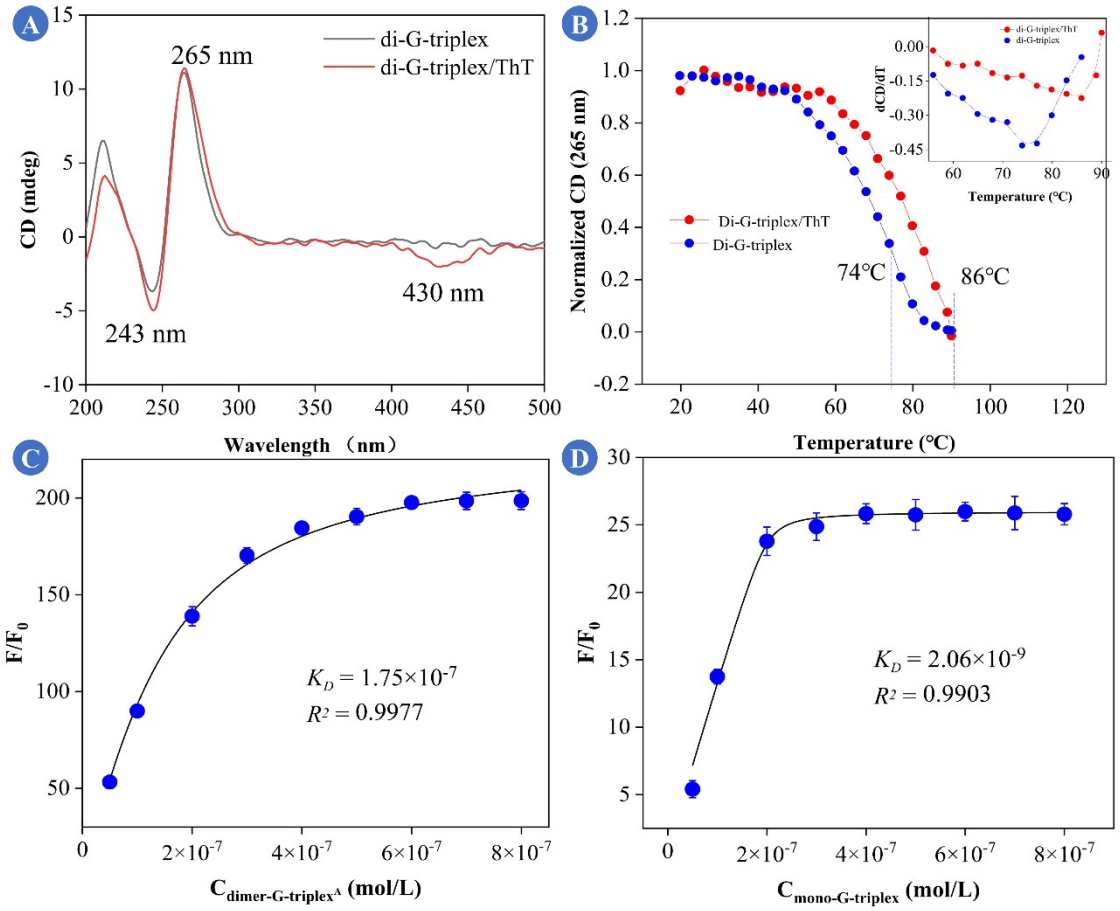

Figure S1. (A) CD spectra of the di-G-triplex^A (10 μM) before and after incubation with ThT (100 μM). (B) Normalized melting curves of di-G-triplex^A (5 μM) and di-G-triplex^A (5 μM) /ThT (25 μM) compound. (C) Fluorometric titration curves of ThT (200 nM) with different concentrations of di-G-triplex^A. (D) Fluorometric titration curves of ThT (200 nM) with different concentrations of mono-G-triplex.

To elucidate the binding mechanism of ThT to di-G-triplex^A, CD spectra were acquired for both di-G-triplexA and di-G-triplexA/ThT complexes. As depicted in **Figure S1A**, the CD spectrum of di-G-triplex^A exhibited a robust positive peak at approximately 265 nm and a corresponding negative peak at 243 nm, characteristics that remained unchanged upon ThT addition. These spectral features are distinct from those of single-stranded DNA (ssDNA) and double-stranded DNA (dsDNA), which

typically display a positive peak near 280 nm, indicative of a parallel G-triplex formation for di-G-triplex^{A} both in the presence and absence of ThT. Furthermore, the presence of a negative CD band around 430 nm in the solution containing both di-G-triplex^{A} and ThT, absent in the di-G-triplex^{A} alone solution, suggests an intercalation mode of ThT binding to di-G-triplex^{A}. This observation aligns well with existing literature on G-triplex structure,[3] thereby corroborating the reliability of our study in elucidating G-triplex structures. Subsequently, the melting temperatures (Tm) of di-G-triplex^{A} and di-G-triplex^{A}/ThT were assessed by monitoring the CD absorbance at 265 nm across a range of temperatures (**Figure S1B**). The Tm of di-G-triplex^{A} was approximately 74°C, notably higher than the reported Tm of 60°C for a mono-G-triplex sequence,[3] indicating the enhanced stability of di-G-triplex^{A} compared to mono-G-triplex structures. Furthermore, upon noncovalent binding with ThT to form a fluorescence probe, the Tm value increased to 86°C, revealing the robust stability of the di-G-triplex-based fluorescence probe at physiological temperatures. Additionally, to assess the binding affinity, we determined the equilibrium dissociation constant (K_d) between ThT and di-G-triplex^{A} to be 1.75×10^{-7} mol/L (**Figure S1C**) through fitting of fluorometric titration curves. This value notably exceeds the K_d value observed between ThT and mono-G-triplex (2.06×10^{-9} mol/L) (**Figure S1D**). The significant enhancement in affinity between ThT and di-G-triplex^{A} suggests a marked improvement in fluorescence output.

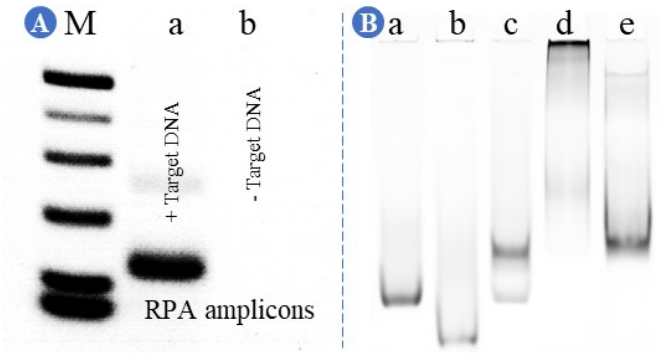

Figure S2. (A) Imaged results of the RPA kit in the absence (b) and presence (a) of target DNA, respectively. (B) Visualized bands of (a) trigger primer, (b) padlock probe, (c) trigger primer, padlock probe, and T4 DNA ligase, (d) trigger primer, padlock probe, T4 DNA ligase, and Klenow polymerase, and (e) trigger primer, padlock probe, T4 DNA ligase, Klenow polymerase, and Nt.BbvCI endonuclease. Experimental conditions: [Trigger primer]=50 nM, [Padlock probe]=50 nM, [T4 DNA ligase]=50 U/mL, [Klenow polymerase]=25 U/mL, [Nt.BbvCI endonuclease]=50 U/mL.

Characterization of Working Mechanism through Gel Electrophoresis. In **Figure S2A**, the operation of the RPA was demonstrated. In the absence of target DNA, lane b exhibited no observable bands. Conversely, a distinct band in lane a was evident, confirming the success of the RPA. To ascertain the capability of the cleaved trigger primer to hybridize with the padlock probe and initiate nRCA, we artificially synthesized the primer to simplify the reaction and assessed its interaction with the padlock probe under various conditions in **Figure S2B**. Lane a and lane b depicted bands representative of the trigger primer and padlock probe, respectively. Their hybridization product after ligation displayed an increased molecular weight in lane c. Upon exposure to Klenow polymerase (lane d), a series of products with a delayed mobility emerged, indicating the progression of RCA. Further treatment of the polymerization products with Nt.BbvCI endonuclease resulted in the generation of nicking products in lane e, affirming the successful operation of nRCA.

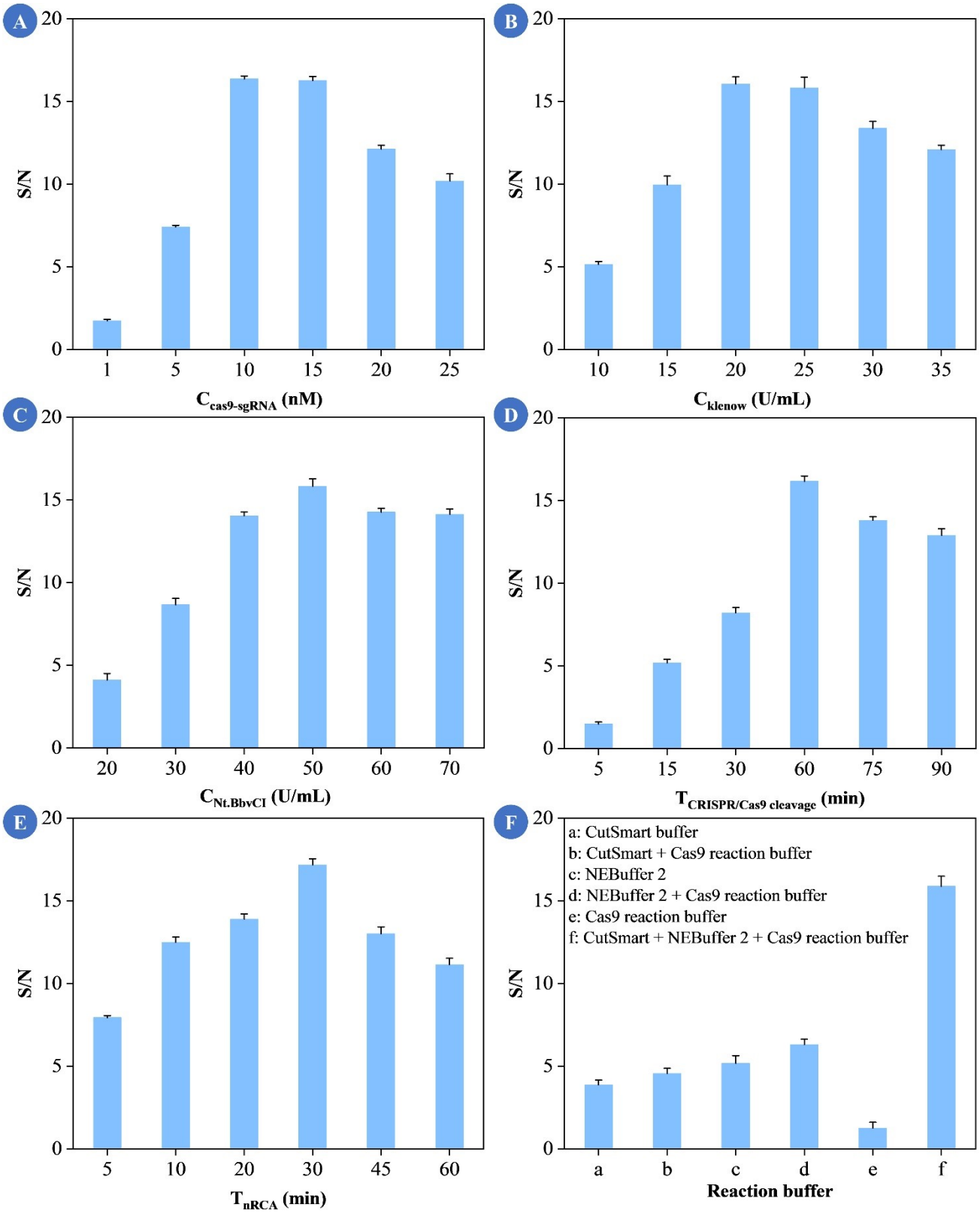

Figure S3. Optimization of Cas9-sgRNA complex concentration (A), Klenow polymerase concentration (B), Nt.BbvCI concentration (C), CRISPR/Cas9 cleavage time (D), nRCA reaction time (E), and reaction buffer (F) on the assay performance. Experimental conditions: (A) [Padlock

probe]=50 nM, [Klenow polymerase]=20 U/mL, [Nt.BbvCI endonuclease]=50 U/mL, [T4 DNA ligase]=50 U/mL, [CRISPR/Cas9 cleavage time]=60 min, [nRCA reaction time]=30 min, [ThT]=1 μM; (B) [Padlock probe]=50 nM, [Cas9]=10 nM, [sgRNA]=10 nM, [Nt.BbvCI endonuclease]=50 U/mL, [T4 DNA ligase]=50 U/mL, [CRISPR/Cas9 cleavage time]=60 min, [nRCA reaction time]=30 min, [ThT]=1 μM; (C) [Padlock probe]=50 nM, [Cas9]=10 nM, [sgRNA]=10 nM, [Klenow polymerase]=20 U/mL, [T4 DNA ligase]=50 U/mL, [CRISPR/Cas9 cleavage time]=60 min, [nRCA reaction time]=30 min, [ThT]=1 μM; (D) [Padlock probe]=50 nM, [Cas9]=10 nM, [sgRNA]=10 nM, [Klenow polymerase]=20 U/mL, [Nt.BbvCI endonuclease]=50 U/mL, [T4 DNA ligase]=50 U/mL, [nRCA reaction time]=30 min, [ThT]=1 μM; (E) [Padlock probe]=50 nM, [Cas9]=10 nM, [sgRNA]=10 nM, [Klenow polymerase]=20 U/mL, [Nt.BbvCI endonuclease]=50 U/mL, [T4 DNA ligase]=50 U/mL, [CRISPR/Cas9 cleavage time]=60 min, [ThT]=1 μM. (F) [Padlock probe]=50 nM, [Cas9]=10 nM, [sgRNA]=10 nM, [Klenow polymerase]=20 U/mL, [Nt.BbvCI endonuclease]=50 U/mL, [T4 DNA ligase]=50 U/mL, [CRISPR/Cas9 cleavage time]=60 min, [nRCA reaction time]=30 min, [ThT]=1 μM.

Optimization of Experimental Conditions. Optimization of experimental conditions is crucial for achieving the best assay performance. Key parameters such as the concentrations of the Cas9-sgRNA complex, Klenow polymerase, and Nt.BbvCI were firstly adjusted in **Figure S3A-C** to enhance the signal-to-noise (S/N) ratio. The optimal concentration for Cas9-sgRNA was determined to be 10 nM (**Figure S3A**), as concentrations below this threshold were insufficient for inducing the subsequent nRCA, while concentrations above resulted in an undesirable increase in background signal. Similarly, the optimal concentrations for Klenow and Nt.BbvCI were identified as 20 U/mL (**Figure S3B**) and

50 U/mL (**Figure S3C**), respectively. These concentrations were found to balance the polymerization and nicking, maximizing signal intensity while minimizing background interference. Subsequently, the reaction times for CRISPR/Cas9 cleavage and nRCA amplification were fine-tuned. **Figure S3D** indicated that increasing the CRISPR/Cas9 cleavage time up to 60 min enhanced the S/N value. Beyond 60 min, however, the S/N ratio decreased due to elevated background signals. Consequently, a CRISPR/Cas9 cleavage time of 60 min was selected. Similarly, **Figure S3E** demonstrated that the optimal reaction time for nRCA is 30 min. Finally, considering the impact of different buffer compositions on the assay, **Figure S3F** illustrated the optimization of the reaction buffer. The combined use of CutSmart buffer, NEBuffer 2, and Cas9 reaction buffer was found to contribute synergistically to the maximal enhancement of the S/N response.

A

Samples	Added (U/mL)	Found (U/mL)	Recovery (%)	RSD (%)
1	10^2	9.27×10^1	92.7	1.53
2	10^3	9.43×10^2	94.3	1.24
3	10^4	9.51×10^3	95.1	1.76
4	10^5	9.68×10^4	96.8	1.35
5	10^6	9.87×10^5	98.7	1.23

B

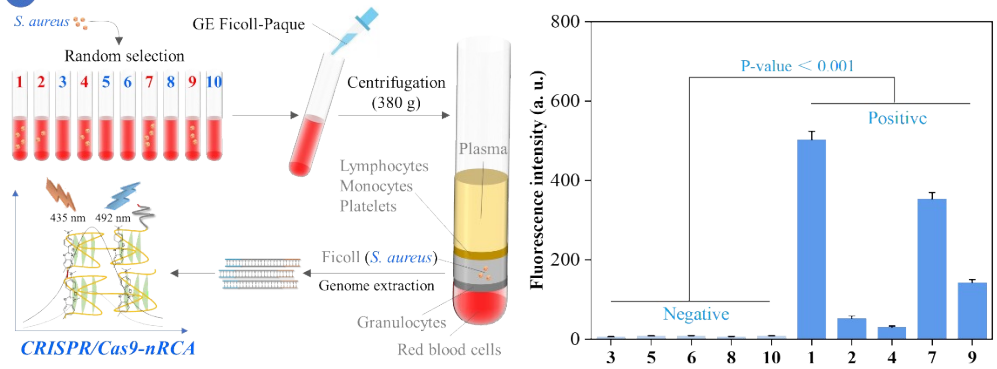

Figure S4. (A) Recovery Rates of *S. aureus* Detection from Spiked Blood Samples (n = 3) and (B) Blind testing of prepared blood samples using CRISPR/Cas9-nRCA to confirm the reliability of accurate identification of *S. aureus*-infected samples (1, 2, 4, 7, and 9). Error bars are obtained from three parallel tests.

Real sample analysis. It's known that *S. aureus* gains entry to the bloodstream through contaminated medical devices, surgeries, and skin infections, leading to severe infections like bacteremia or septicemia. In the evaluation of the RPA-CRISPR/Cas9-nRCA detection system, varying *S. aureus* concentrations were spiked into blood samples from healthy donors. After centrifugation, genomic DNA extraction, and testing, the system, utilizing di-G-triplex[A], demonstrated favorable recovery rates across various *S. aureus* concentrations in **Figure S4A**. Blind testing of ten samples in **Figure S4B**, including five spiked with *S. aureus*, accurately identified infected samples (1, 2, 4, 7, and 9), aligning

precisely with pre-established blind sample results. These findings strongly support the practicability of the current method for analyzing real biological samples, indicating its potential utility in clinical settings for accurate and early detection of *S. aureus*.

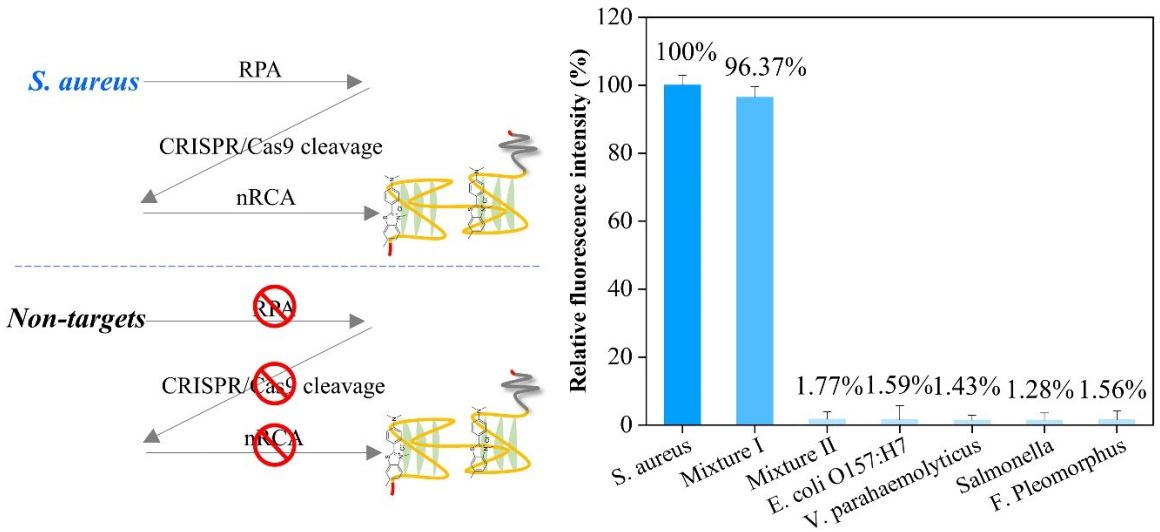

Figure S5. Fluorescence responses of various pathogens (1.0×10^6 CFU/mL) and their mixtures, with Mixture I containing *S. aureus* and Mixture II excluding it. Error bars represent three parallel tests. The response of target *S. aureus* (F_t-F_0) is set at 100%, while the relative fluorescence response of other analytes is calculated as $[(F-F_0)/(F_t-F_0)] \times 100\%$, where F, F_t, and F_0 denote the peak fluorescence of non-targets, target, and the control, respectively.

Specificity study. To assess specificity, various pathogens, including *S. aureus*, *E. coli* O157:H7, *V. parahaemolyticus*, *Salmonella, F. Pleomorphus*, and their mixture were subjected to measurement. As depicted in **Figure S5**, the CRISPR/Cas9-nRCA system exhibited a significant increase in fluorescence exclusively in the presence of *S. aureus*. In contrast, all non-target species exhibited negligible fluorescent signal increments comparable to the blank control devoid of pathogens. This outcome is attributed to the dual effects of RPA's selective amplification and CRISPR/Cas9's precise DNA targeting and cleavage. Consequently, only the *S. aureus* triggers the continual formation of di-G-triplex^A, substantiating the excellent specificity of the method.

Table S1. Comprehensive list of oligonucleotides utilized in the experimental procedures.

Items	Sequences (5' to 3' order)
mono-G-triplex	TGGGTAGGGCGGG
di-G-triplex	TGGGTAGGGCGGGTGGGTAGGGCGGG
di-G-triplex^{A}	TGGGTAGGGCGGGaaaaaaTGGGTAGGGCGGG
di-G-triplex^{G}	TGGGTAGGGCGGGgggggggTGGGTAGGGCGGG
di-G-triplex^{C}	TGGGTAGGGCGGGccccccTGGGTAGGGCGGG
di-G-triplex^{T}	TGGGTAGGGCGGGttttttTGGGTAGGGCGGG
Padlock probe for di-G-triplex^{A}	P-TGCTCATTGCTGA***GGCCCGCCCTACCCA***TTTTTT***CCCGCCCTACCC A***TCTTCAATCTTT
Padlock probe for mono-G-triplex	P-TGCTCATTGCTGA***GGCCCGCCCTACCCA***TTTTTTTTTTTTTTTTTTT TTCTTCAATCTTT
RPA-FP	AAAAAAGCACATAACAAGCG
RPA-RP	GATAAAGAAGAAACCAGCAG
Scaffold template	GTTTTAGAGCTAGAAATAGCAAGTTAAAATAAGGCTAGTCCGTTAT CAACTTGAAAAAGTGGCACCGAGTCGGTGCTTTT
Primer for Scaffold template	AAAAGCACCGACTCGGTGCC
Target-specific template	CCTCTAATACGACTCACTATAGGAATGAGCAAAAGATTGAAGAGT TTTAGAGCTAGA

The complementary sequences between "Scaffold template" and "Primer for Scaffold template" are underlined. The RPA primers used in this study were designed based on methods outlined in previous reports.[4]

Table S2. Comparison of the Current CRISPR/Cas9-nRCA with Previously Reported Methods for Pathogen Detection.

Methods	LOD	Linear range	Orders of amplification	Ref.
Bacteria culture	/	> 720	/	[5]
PCR	64	10^3–10^7	5	[6]
Immunosensors	2.6	10^3–10^8	6	[7]
Molecular standard for positive quality control	50	50–10^7	7	[8]
SPR	1.5×10^3	10^2–10^5	4	[9]
Fluorescence	10	10–10^6	6	[10]
Electrochemistry	2.4×10^2	1.8×10^3–1.8×10^7	5	[11]
SERS	13	4.3×10–4.3×10^7	7	[12]
Colorimetry	11	5×10^2–5×10^4	3	[13]
Lateral flow assay	10^3	10^3–10^8	6	[14]
Chemiluminescence	2.9×10^2	10^3–10^7	5	[15]
This study	6	10–10^7	7	/

References

1. F. H. Stootman, D. M. Fisher, A. Rodger and J. R. Aldrich-Wright, *Analyst*, 2006, **131**, 1145-1151.
2. X. Xie, B. Choi, E. Largy, R. Guillot, A. Granzhan and M. P. Teulade-Fichou, *CHEM-EUR J.*, 2013, **19**, 1214-1226.
3. H. Zhou, Z.-F. Wu, Q.-J. Han, H.-M. Zhong, J.-B. Peng, X. Li and X.-L. Fan, *Anal. Chem.*, 2018, **90**, 3220-3226.
4. H. Wang, Q. Wu, C. Yan, J. Xu, X. Qin, J. Wang, W. Chen, L. Yao, L. Huang and P. Qin, *Sensor. Actuat. B-Chem.*, **2022**, 369, 132293.
5. S. OHara, *J. Clin. Microbiol.*, 2008, **46**, 3181.
6. L. Hu, B. Han, Q. Tong and D. Cao, *CAN. J. INFECT. DIS. MED.*, 2020, **2020**.
7. J. C. Soares, A. C. Soares, M. Popolin-Neto, F. V. Paulovich, O. N. Oliveira Jr and L. H. C. Mattoso, *Sensors and Actuators Reports*, 2022, **4**, 100083.
8. Y. Feng, D. Zhou, L. Gao and F. He, *Biosens. Bioelectron.*, 2020, **168**, 112527.
9. N. Idil, M. Bakhshpour, I. Perçin and B. Mattiasson, *Biosensors*, 2021, **11**, 140.
10. S. Yao, C. Zhao, M. Shang, J. Li and J. Wang, *Food Chem. Toxicol.*, 2021, **150**, 112071.
11. E. Han, X. Li, Y. Zhang, M. Zhang, J. Cai and X. Zhang, *Anal. Biochem.*, 2020, **611**, 113982.
12. A. Zhu, S. Ali, Y. Xu, Q. Ouyang and Q. Chen, *Biosens. Bioelectron.*, 2021, **172**, 112806.
13. J. Zhang, Y. Fan, J. Li, B. Huang, H. Wen and J. Ren, *Biosens. Bioelectron.*, 2022, **217**, 114716.
14. M. Zhao, X. Yao, S. Liu, H. Zhang, L. Wang, X. Yin, L. Su, B. Xu, J. Wang and Q. Lan, *Food Chem.*, 2021, **339**, 127955.
15. E. Fan, J. Peng, Y. He, Y. Wu, H. Ouyang, Z. Xu and Z. Fu, *Sensor. Actuat. B-Chem.*, 2019, **285**, 271-276.